

Effects of Ionizing Radiation on the  
Transport Chemistry of Cesium Iodide

R. W. Elrick and D. A. Powers

Sandia National Laboratories  
Albuquerque, NM, USA

ABSTRACT

Mixtures of cesium iodide or silver iodide vapors in steam and hydrogen at 1170K were passed over stainless steel in a radiation field produced by a  $^{60}\text{Co}$  source. Cesium iodide and silver iodide were observed to dissociate. The iodine passed through the system. Cesium was found to have bound to oxide layers on the stainless steel. Dissociation of iodide vapors and cesium reaction were not observed in similar experiments done without a radiation field.

Thermochemical analyses of the Cs-I-O-H system in the presence of ionizing radiation are presented and used to explain the reactions of cesium iodide.

INTRODUCTION

During severe reactor accidents, radionuclides released from degrading reactor fuel must pass through the reactor coolant system before they can contribute to the threat to public safety. The ability of vaporized radionuclides to negotiate passage through the reactor coolant system is strongly dependent on the chemical interactions of the radionuclides with materials present along the flow pathway. The chemical environment encountered by the radionuclides in the reactor coolant system during a severe accident is far more hostile than that commonly encountered in laboratory chemistry studies. This environment may involve high pressures (over 100 atmospheres) and strongly oxidizing or strongly reducing conditions. Always high temperatures and intense radiation fields would be expected.

For several years, the U. S. Nuclear Regulatory Commission has sponsored at Sandia National Laboratories a program to investigate the chemistry that might affect transport of radionuclides during severe reactor accidents (1). Experimental studies of the rates of deposition of CsOH (2), CsI (3), and Te (4) on stainless steel have been conducted as part of this research effort. These experimental studies have involved attempts to produce prototypic thermal and

8603040139 860113  
PDR FOIA  
SHOLLY85-804 PDR

ITEM  
C  
3

chemical environments. Intense radiation fields that would also be expected in the coolant system of a reactor during an accident were not included in these studies.

Recently, a series of experiments to examine cesium iodide transport was done in a radiation field (5). In this paper, the results of these experiments and some discussion of their implications for the chemistry of iodine during severe reactor accidents are presented.

#### EXPERIMENTAL APPARATUS AND PROCEDURES

The experimental procedures and apparatus were similar to those employed in previous studies without a radiation field (2,3). The apparatus was the Fission Product Reaction Facility which is shown schematically in Figure 1 and has been described elsewhere (2). The apparatus was located for these experiments in Sandia's Gamma Irradiation Facility (GIF) which uses a 130000 curie  $^{60}\text{Co}$  source to produce an intense radiation field.  $^{60}\text{Co}$  gamma rays are peaked at energies of 1.173 and 1.332 Mev. In typical experiments, a flow of steam at a pressure somewhat above ambient is introduced at the rate of 0.04 moles/min to the super heater. Reactions of the steam with Inconel or stainless steel liners in the apparatus create a hydrogen partial pressure, or hydrogen may be introduced to the flow.

Cesium iodide or silver iodide vapors are introduced in a helium carrier gas to the flow as it emerges from the super heater. The vapor mixture then passes through an isothermal ( $\pm 5\text{K}$ ) test section about 1/2 meter long. The inside diameter of the piping system through the apparatus is 2.6 cm.

Within the test section, the vapor mixture passes over type 304 stainless steel coupons. These coupons are variously treated:

- (1) as received (c)
- (2) cold-worked by glass bead peening (P)
- (3) pre-oxidized at 1270K for 1 hour ( $\text{O}_1$ )
- (4) pre-oxidized at 1170K for 2 hours ( $\text{O}_2$ )
- (5) pre-oxidized at 1170K for 4 hours ( $\text{O}_3$ )

Also, for some of the experiments in the radiation field silver-plated copper coupons (s) were located in the test section. Reference coupons are located upstream of the point iodide vapors are introduced.

The flow emerges from the test section into a condenser. An automatic sampler allows sequential samples of the condensate to be taken for subsequent analyses. A mass spectrometer is used to determine the hydrogen, helium and argon (a buffer and calibrating gas for hydrogen) gases in the flow.

Tests 40, 41, and 42 were done in the radiation field. The conditions of these tests are shown in Table 1. Results of these experiments will be compared to results of tests 18 and 35 which are also described in Table 1 and were done without a radiation field being present. Test 40 involved CsI vapors in steam and hydrogen passing over stainless steel and silver plated copper coupons. Test 41 was similar except silver iodide vapors were involved. Test 42 was similar to test 40 and used CsI vapors, but no silver coupons were present.

Radiation intensities were measured using thermoluminescent dosimeters arrayed as shown in Figure 2. The peak radiation intensity was found to be 1610 rads/min. The radiation intensity fell by about 400 rads/min across the apparatus width. Microprobe analyses that are reported are for as-received coupons exposed to a field of 1430 to 1020 rads/minute.

#### RESULTS OF THE EXPERIMENTS

The most immediate results of the experiments came from the analyses of steam condensate samples which are summarized in Table 2. Condensate from test 18 and test 35, which were done without a radiation field, contained about equal parts of cesium and iodine as determined by atomic adsorption spectroscopy and ion chromatography, respectively. This is the expected result since cesium and iodine are introduced as CsI. Condensate from tests 40 and 42, which were done in a radiation field, contained about 5 to 10 times as much iodine as cesium. Test 41, which involved AgI vapors, produced condensate containing more than 1000 times as much iodine as silver.

It is apparent from these few results that iodide vapors were being affected by the radiation field. The effect is to cause CsI (and, apparently, AgI) to dissociate in a manner that permitted the cesium to be retained preferentially in the test apparatus, but with an iodine species free to pass into the condenser and to be collected in the condensate.

To ascertain where the cesium was retained, several of the as-received stainless steel coupons exposed to the vapors were examined by x-ray fluorescence and electron microprobe. X-ray fluorescence did not show more than background levels of either cesium or iodine on the surfaces of the coupons. This result is analogous to that obtained in tests without a radiation field present. Electron micrographs of sectioned specimens did show cesium was present in the oxide. But, the cesium was found deep within the oxide layer on the coupons.

Results of electron microprobe analyses of coupons from tests 18 and 40 are shown in Figures 3 and 4, respectively. The oxide on the coupon from test 18 (CsI vapors without a radiation field present) consists of two layers. The outer layer is  $Fe_3O_4$  containing about 2 percent manganese. The inner layer is an iron-chromium inverse spinel phase containing some metallic inclusions composed of iron and nickel. Both layers are free of cesium and iodine to the limits of detectability defined by the instrument background ( $\sim 0.05$  wt. % Cs).

The oxide layer on stainless steel exposed to gamma radiation in test 40 was different. It was a triplex structure. The outer two layers were similar to the two layers found on the stainless steel in test 18 with a radiation field present. That is, the outermost layer was  $Fe_3O_4$ . The middle layer was an iron-chromium oxide. The third oxide layer has been found only in tests with a radiation field. This layer is rich in chromium, manganese, and silicon. It seems very tightly adhered to the metal.

Cesium was found at concentrations of up to 1 wt. % in the middle oxide layer on the coupons from tests with a radiation field present. The disposition of cesium in the oxide layer can be seen more clearly in the plot of concentration against position in Figure 5. In this figure, position is measured from the external surface of the specimen. The approximate boundaries of the oxide layers are marked and numbered in the figure. The metallic material is labelled "M". Concentrations of silicon (Si) and manganese (Mn) as well as cesium (Cs) are shown in the figure.

The tendency for cesium to collect in the inner oxide layers on stainless steel has been observed in previous tests with CsOH vapors done without a radiation field present (2). Electron micrography of the coupons from these tests established a correspondence between the locations of cesium and silicon in the inner oxide layer. This correspondence has led Elrick and Sallach to propose  $Cs_2Si_4O_9$  forms within the oxide layer (6).

Attempts to quantitatively analyze the results of electron micrography of samples from the tests of CsI interactions with stainless steel in a radiation field have not yielded a definitive correlation of silicon and cesium. It is, then, not clear that reactions of cesium dissociated from CsI in a radiation field are identical to reactions of CsOH vapors with the oxide in the absence of the field. It is apparent, though, that the reactions are similar and that cesium reaction with the oxide is responsible for cesium retention in the test apparatus when a radiation field is present.

#### THERMOCHEMISTRY OF THE Cs-I-O-H SYSTEM

Elrick and Sallach (7) and Garisto (8) have analyzed the gas phase speciation of the Cs-I-O-H system. The examinations have proved useful in the analysis of the chemical behavior of the Cs-I-O-H system under laboratory conditions. Neither of these examinations considered ions and ionization. The effects of an intense radiation field ought to include the formation of ions in the gas phase. Therefore, our first steps in the analysis of the experiment results has been to re-examine the gas phase speciation of the Cs-I-O-H system including ion formation.

The number of gas phase species that must be considered in the analysis of the Cs-I-O-H system expands considerable when ions are included. The species considered in the analyses here are listed in Table 3. Gibbs free-energies for these species were calculated using the equation:

$$G(T) = \Delta H_f(298) - T\phi(T)$$

where  $\Delta H_f(298)$  is the enthalpy of formation at 298.15K and  $\phi(T)$  is the free-energy function:

$$\phi(T) = -[G(T) - H_o(298)]/T$$

The free-energy functions were themselves calculated from the correlation expression:

$$\phi(T) = A[1] + A[2]X + A[3]X^2 + A[4]X^3 + \\ A[5]\ln(X) + A[6]/X + A[7]X\ln(X)$$

where  $X = T/10,000$ . Parametric values for these correlations are listed in Table 3. For many of the species, values of the free-energy functions were available from standard sources (9). When this was the case, parametric values were determined by non-linear least squares fitting of the above correlation to tabulated values at 298.15K and at 100K intervals between 300 and 3500K. The correlations will reproduce the tabulated values to within  $\pm 0.001$  Gibbs/mole-K.

Thermodynamic properties have not been tabulated for many of the species in Table 3, especially some of the ionic species. For these species, the thermodynamic properties were determined as follows:

CsH(g): Thermodynamic properties were calculated using the rigid-rotor, anharmonic oscillator model (10) and spectroscopic data cited by Huber and Hertzberg (12). The enthalpy of formation is that cited by Wagman et al. (11).

CsI<sup>+</sup>(g): Thermodynamic properties were calculated using structural and vibrational data for CsI(g) and electronic data for CsI<sup>+</sup>(g) (12). The enthalpy of formation was taken to be the average of values cited by Franklin et al. (13) and should be considered quite uncertain.

Cs<sub>2</sub>I<sup>+</sup>: Thermodynamic properties were calculated for a linear rigid-rotor, harmonic oscillator using structural and vibrational data calculated by Milne and Cubicciotti (14). The molecule was assumed to have a <sup>2</sup>Σ ground state. The enthalpy of formation, 70 kcal/mole, is the average of values cited by Franklin et al. (13). Recent work (18,19) seems to favor a lower value, 38-40 kcal/mole, though the evidence is equivocal.

Cs<sub>2</sub><sup>+</sup>(g): Thermodynamic properties were calculated for a rigid rotor-anharmonic oscillator using structural and vibrational data for Cs<sub>2</sub>(g) (9). The electronic ground state was taken to be <sup>2</sup>Σ. The enthalpy of formation is that cited by Wagman et al. (11).

CsO<sub>2</sub>(g): Free-energy function values were calculated from a correlation found by Garisto (8) and these values were fit to the functional form used here. Garisto's estimate of the enthalpy of formation has been adopted.

HI<sup>+</sup>(g): Thermodynamic properties were calculated for a rigid rotor-anharmonic oscillator using spectroscopic and structural data cited by Huber and Hertzberg (12). The enthalpy of formation is taken from Wagman et al. (11).

H<sub>2</sub>O<sup>+</sup>(g): Thermodynamic properties were calculated using structural and vibrational data for H<sub>2</sub>O(g). The electronic ground state was taken to be a doublet. The enthalpy of formation is from Wagman et al. (11).

I<sup>+</sup>(g): Thermodynamic properties were calculated using a conventional statistical mechanics model and the 121 energy levels between the ground state and the dissociation limit (15). The enthalpy of formation is that cited in reference 11.

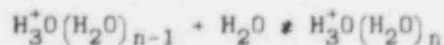
I<sup>-</sup>(g): This ion is isoelectronic with Xe(g). Its thermodynamic properties were calculated assuming a ground state singlet and no excited states up to the dissociation limit. The enthalpy of formation is from reference 11.

I<sub>2</sub><sup>-</sup>(g): The thermodynamic properties were calculated from spectroscopic data cited by Huber and Hertzberg (12). The enthalpy of formation was calculated from the dissociation energy, 24 kcal/mole and collateral data for I(g) and I<sup>-</sup>(g).

I<sub>2</sub><sup>+</sup>(g): The thermodynamic properties were calculated for a rigid rotor-anharmonic oscillator using spectroscopic data (12). The enthalpy of formation is from reference 11.

H<sub>2</sub>O<sub>2</sub><sup>+</sup>, HO<sub>2</sub><sup>+</sup>, and O<sub>3</sub><sup>+</sup>: Free-energy functions for the neutral molecules were assumed for the ions. The enthalpies of formation are those cited by Franklin et al. (13).

No attempt was made to include in the calculations more exotic cesium iodide ions such as Cs<sub>3</sub>I<sub>2</sub><sup>+</sup>, CsI<sub>2</sub><sup>-</sup> or Cs<sub>2</sub>I<sub>3</sub><sup>-</sup> which have been reported (18,19). Nor has hydration of the ions such as the hydration of the hydronium ion (17):



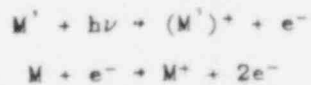
$$n = 1 \text{ to } 7$$

been considered. Such hydrates become of decreasing importance with increasing temperature. The hydrates are more stable, however, in high pressure steam. The presence of hydrates in a reactor coolant system cannot be totally discounted. Significant hydrate formation will affect the validity of the ideal gas assumption invoked below.

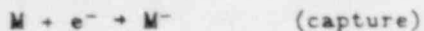
Further details on the thermodynamic properties of species considered here will be published in a Sandia National Laboratories report (16).

The gas phase speciation of the Cs-I-O-H system in the absence of a radiation field was calculated assuming all species were ideal gases. Conventional equilibrium methods were used except an additional charge neutrality constraint was imposed. Results of such a calculation are shown in Figure 6 for a system at one atmosphere total pressure and having a hydrogen-to-steam ratio of 0.1 and a Cs/H ratio of  $4.95 \times 10^{-4}$ . The source of cesium was taken to be CsI. The predominant vapor species is, as expected, CsI(g). Ions are present. Cs<sup>+</sup>(g) and I<sup>-</sup>(g) are the most abundant ions. (On the scale of the plot, the partial pressures of these ions are nearly indistinguishable.) It is apparent, however, that for most purposes the contributions of ions to the gas phase speciation is negligible.

Gamma ray interactions with materials will free electrons. Primary electrons produced by Compton scattering of <sup>60</sup>Co gamma rays have a mean energy of about 0.5 Mev. Simple shielding calculations indicate these electrons (delta rays) in the tests considered here come primarily from the interaction of gamma rays with structural elements of the test apparatus rather than direct interaction of gamma rays with the vapor phase. The highly energetic primary electrons will interact with vapor species to free additional electrons in a reaction chain:



This chain propagates until electron energies become too low to induce ionization. The ions that are formed can participate in various charge exchange reactions while the low energy electrons can be captured:



Finally, ions can be neutralized:



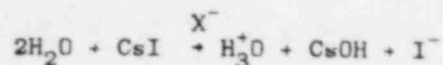
The formation, charge exchange and neutralization reactions of ions all proceed at finite rates. These rates are not known, in general. They are, however, dependent on the radiation dose rate, natures of the ions, and the geometry of the system. The charge exchange and neutralization processes tend to move the system toward thermal equilibrium speciation. This is frustrated by the continuous bombardment by gamma rays, primary electrons and the shower of secondary electrons.

If it is assumed that a steady state is achieved and that the processes of ion formation and evolution are fast in comparison to the neutralization processes, the system will establish a dynamic equilibrium. This will not be a true chemical equilibrium since it will be dependent on system geometry, etc. Some insight into the nature of speciation during this dynamic equilibrium can be gained by considering the system to be equilibrated except ion populations are shifted to higher levels by the continuous bombardment. The ion population can be quantitatively characterized by the so-called "dynamic charge separation,"  $M_C$ , which is defined by:

$$M_C = \sum_{+}(i) = \sum_{-}(i)$$

where  $\sum_{+}(i)$  and  $\sum_{-}(i)$  are the total moles of positively and negatively charged species in the system.  $M_C$  has, of course, finite values even in the absence of a radiation field. For the system described by Figure 6,  $M_C$  varies between  $10^{-11}$  and  $10^{-7}$  as  $T$  varies from 1000 to 1600K. Under the action of the radiation field,  $M_C$  is increased. Speciation of the system can be estimated using the definition of  $M_C$  in place of the normal charge neutrality constraint. (Note, however, that the definition of  $M_C$  still enforces overall electrical neutrality.)

Results of a calculation for the system described above except  $M_c = 10^{-3}$  are shown in Figure 7. Ions, especially  $H_3O^+$  and  $I^-$  are the dominant contributors to the vapor speciation aside from  $H_2O(g)$  and  $H_2(g)$ . The most important cesium species is  $CsOH(g)$ . The effect of radiation on the system is then, apparently, promotion of the over all reaction:



where  $X^-$  simply designates some ion source. Increasing the hydrogen-to-steam ratio to 10 or the system pressure to 100 atmospheres does not alter this as the dominant reaction. At higher hydrogen concentrations, formation of  $Cs(g)$  rather than  $CsOH(g)$  does make a significant contribution to the speciation. Incremental changes in the dynamic charge separation,  $M_c$ , from thermal values shows that the cesium hydroxide partial pressure is nearly directly proportional to  $M_c$ .

The results of the tests of  $CsI$  transport in a radiation field can be understood in terms of the vapor speciation shown in Figure 7. The effect of radiation is to increase the vapor concentration of  $CsOH(g)$  which can react with oxidizing stainless steel as observed in earlier experiments (2). This removes cesium from the gas phase so that reformation of  $CsI(g)$  cannot occur when the gas phase emerges from the radiation field.

The calculated speciation also suggests the disposition of iodine freed by the dissociation of  $CsI(g)$ . This iodine is present predominantly as  $I^-(g)$ . The vapor concentrations of  $I(g)$  and  $I_2(g)$  are kept quite low. At these low iodine concentrations, formation of other metal iodides such as  $FeI_2(g)$  and  $NiI_2(g)$  will be quite limited. Though not examined here, it is likely that formation of organic iodides will also be inhibited by the low partial pressures of  $I(g)$  and  $I_2(g)$ .

#### CONCLUSIONS

Experiments have shown that radiation fields can affect the transport chemistry of  $CsI$ . The effect is to liberate iodine and to trap cesium in the oxide layers on stainless steel in the flow pathway. Thermochemical analyses suggest the liberated iodine will be present predominantly as  $I^-(g)$  and largely unavailable for reaction with other metals to form vapor phase metal iodides.

These results can have significant ramifications on the expected behavior of radionuclide iodine and cesium under accident conditions. The results also imply radiation is an important constituent of the chemical environment of the reactor coolant system under accident conditions. The effects of radiation and the ionization it induces ought to be considered in the development of models of radionuclide behavior during severe reactor accidents.

#### References

1. High Temperature Fission Product Chemistry Program, NRC FINA 1227, L. Chan, Program Monitor, Fuel Systems Branch, Office of Nuclear Regulatory Research, USNRC.
2. R. M. Elrick, R. A. Sallach, A. L. Ouellette, and S. C. Douglas, Reaction Between Some Cesium-Iodine Compounds and the Reactor Materials 304 Stainless Steel, Inconel 600 and Silver, Volume I Cesium Hydroxide Reactions, NUREG/CR-3197/1 of 3, SAND83-1395, Sandia National Laboratories, Albuquerque, NM, June, 1984.
3. R. A. Sallach, R. M. Elrick, S. C. Douglas, and A. L. Ouellette, Reaction Between Some Cesium-Iodine Compounds and the Reactor Materials 304 Stainless Steel, Inconel 600 and silver, Volume II Cesium Iodide Reactions, NUREG/CR-3197/2 of 3, SAND83-0395, Sandia National Laboratories, Albuquerque, NM.
4. R. A. Sallach, C. J. Greenholdt and A. R. Taig, Chemical Interactions of Tellurium Vapors with Reactor Materials, SAND82-1145, NUREG/CR-2921, Sandia National Laboratories, Albuquerque, NM, March, 1984.
5. R. M. Elrick, R. A. Sallach and A. L. Ouellette, Effect of Ionizing Radiation on the Chemistry of the CsI-Steam-Hydrogen-304 Stainless Steel System-A Preliminary Report, Sandia National Laboratories, Albuquerque, NM.
6. R. M. Elrick and R. A. Sallach, "Fission Product Chemistry in the Primary System," paper TS4.6, Proc. Int'l Meeting on LWR Severe Accidents Evaluation, Cambridge, Mass., August 28-September 1, 1983.

7. R. W. Elrick and R. A. Sallach, "Fission Product Chemistry in the Vapor State," Chapter 5.2 in Technical Bases for Estimating Fission Product Behavior During LWR Accidents, NUREG-0772, U. S. Nuclear Regulatory Commission, Washington, DC, June 1981.
8. F. Garisto, Thermodynamics of Iodine, Cesium, and Tellurium in the Primary Heat-Transport System Under Accident Conditions, AECL-7782 Atomic Energy of Canada, LTD, Pinawa, Manitoba, Canada, November, 1982.
- 9a. D. R. Stull and H. Prophet, JANAF Thermochemical Tables, 2nd Edition, NSRDS-NBS 37, National Bureau of Standards, June, 1971.
- b. M. W. Chase et al., J. Phys. Chem. Ref. Data 3 (1974) 311.
- c. M. W. Chase et al., J. Phys. Chem. Ref. Data 4 (1975) 311.
- d. M. W. Chase et al., J. Phys. Chem. Ref. Data 11 (1982) 311.
10. Mayer and Mayer, Statistical Mechanics, John Wiley and Sons, 1940.
11. D. D. Wagman et al., J. Phys. Chem. Ref. Data, Vol. 11, Supplement No. 2, 1982.
12. K. P. Huber and G. Herzberg, Molecular Spectra and Molecular Structure IV. Constants of Diatomic Molecules, Van Nostrand Reinhold Co., 1979.
13. J. L. Franklin, J. G. Dillard, H. M. Rosenstock, J. T. Herron, K. Draxl, and F. H. Field, Ionization Potentials, Appearance Potentials, and Heats of Formation of Gaseous Positive Ions, NSRDS-NBS 26, National Bureau of Standards, Washington, DC, June, 1969.
14. T. A. Milne and D. Cubicciotti, J. Chem. Phys. 30 (1959) 1418.
15. C. E. Moore, Atomic Energy Levels, U. S. Nat'l Bureau of Stds. Circ. 467, 1949.
16. D. A. Powers, Thermodynamic Properties of Some Species in the Cs-I-O-H System, Sandia National Laboratories, Albuquerque, NM in preparation.

17. P. Kebarle and A. M. Hogg, J. Chem. Phys. **42** (1965) 798.
18. I. V. Sidorova, A. V. Gusarov and L. N. Gorokhov, Int'l J. Mass Spectroscopy and Ion Physics **31** (1979) 367.
19. Yu. Ya. Rybkin, A. V. Gusarov and L. N. Gorokhov, Theoretical and Experimental Chemistry **15** (1979) 465.

Table 1

Experiment Conditions

Laboratory Tests

Test 18	CsI vapor/steam +H <sub>2</sub> /304SS coupons
Test 35	CsI vapor/steam + H <sub>2</sub> /304SS + Ag coupons

GIF Tests

Test 40	CsI vapor/steam +H <sub>2</sub> /304SS + Ag coupons
Test 42	CsI vapor/steam +H <sub>2</sub> /304SS coupons
Test 41	AgI vapor/steam +H <sub>2</sub> /304SS + Ag coupons

	<u>Test 18</u>	<u>Test 35</u>	<u>Test 40</u>	<u>Test 42</u>	<u>Test 41</u>
Run duration (hrs)	3	3	9	9	9
Nominal steam flow rate (mole/min)	0.04	0.04	0.04	0.04	0.04
Superheater temp (K)	1370	1240	1270	1260	1320
Reaction tube temp (K)	1270	1170	1170	1170	1170
Nominal flow rate of species (mole/min)	CsI 5 × 10 <sup>-6</sup>	AgI 5 × 10 <sup>-6</sup>			

Table 2

Analysis of Steam Condensate Samples. Cesium and Silver Determined by Atomic Absorption Spectroscopy; Iodine Determined by Ion Chromatography.

		<u>Cesium (ppm)</u>	<u>Iodine (ppm)</u>
<u>No Field</u>			
Test 18	CsI/304SS	~1000	~1000
Test 35	CsI/304SS + Ag	~1000	~1000
<u>Field</u>			
Test 40	CsI/304SS + Ag	155	1500
Test 42	CsI/304SS (no Ag)	290	1000
		<u>Silver (ppm)</u>	
Test 41	AgI/304SS + Ag	<0.1	700

Table 3

Correlation Parameters Used to Calculate Gibbs Free Energy

Parameters\*

Species	A[1]	A[2]	A[3]	A[4]	A[5]	A[6]	A[7]	$\Delta H_f(298)$ (ca./mole)	Ref
1. H <sub>2</sub> O	71.5353	49.6806	-78.0775	32.7719	9.33660	0.247391	31.9148	-57798	9d
2. H <sub>2</sub>	52.4946	9.08877	-11.7388	-0.415187	7.89367	0.218718	11.0344	0	9d
3. O <sub>2</sub>	57.857	0.0312473	15.5420	-1.78969x10 <sup>-3</sup>	4.72389	0.178176	-16.7050	0	9d
4. H	5.17062	-135.714	317.063	-192.163	-3.40325	0.0527043	-117.136	52103	9d
5. OH	70.0373	25.8297	-48.5113	17.3238	9.09452	0.239950	26.2917	9318	9d
6. O	53.7172	4.11753	-10.7695	4.75467	5.72452	0.160236	5.99812	59554	9d
7. HO <sub>2</sub>	-3.94422	-243.968	606.851	-360.074	-11.0345	0.0235491	-243.659	5000	9d
8. H <sub>2</sub> O <sub>2</sub>	37.1605	-83.1478	231.520	-91.6313	-0.482166	0.192705	-120.478	-32530	9a
9. O <sub>3</sub>	46.0284	-50.4520	146.180	-60.5335	+0.922293	0.189177	-89.0097	34200	9a
10. H <sub>2</sub> O <sup>+</sup>	72.4179	49.7575	-79.4254	34.5683	9.21042	0.245271	31.1464	234600	+
11. H <sub>3</sub> O <sup>+</sup>	57.2476	48.1810	-42.2018	20.1083	5.62504	0.208926	-0.274354	138900	9a
12. H <sup>+</sup>	39.1787	2.39819	-5.55621	3.14605	5.13533	0.150166	2.19440	367171	9d
13. H <sub>2</sub> <sup>+</sup>	54.9794	36.8365	-65.4733	36.8378	7.62433	0.208639	21.3416	357235	9d
14. H <sub>2</sub> <sup>-</sup>	45.1096	9.10133	-1.98798	5.79897	5.17864	0.183035	-9.57394	56255	9d
15. O <sup>-</sup>	52.2717	2.84047	-7.58038	3.17474	5.54790	0.157599	4.39616	24322	9d
16. O <sup>+</sup>	49.0997	-1.43070	3.33468	-1.93317	4.87163	0.146946	-1.28090	374949	9d
17. O <sub>2</sub> <sup>-</sup>	55.5894	-16.6177	50.6145	-20.3134	4.13020	0.181946	-31.8083	-11614	9d
18. O <sub>2</sub> <sup>+</sup>	64.3941	20.6636	-30.9175	19.7863	6.19705	0.192267	3.84846	279349	9d
19. OH <sup>+</sup>	68.6953	35.0211	-65.6889	30.0036	8.69386	0.223516	28.4665	314800	9b
20. OH <sup>-</sup>	65.4639	23.2657	-42.3597	15.7772	8.57888	0.224872	22.2769	-34320	9b
21. H <sub>2</sub> O <sub>2</sub> <sup>+</sup>	37.1605	-83.1478	231.520	-91.6313	-0.482166	0.192705	-120.478	212000	+
22. HO <sub>2</sub> <sup>+</sup>	-3.94422	-243.968	606.851	-360.074	-11.0345	0.0235491	-243.659	271000	+
23. O <sub>3</sub> <sup>+</sup>	46.0284	-50.4520	146.180	-60.5335	0.922293	0.189177	-89.0097	318000	+
24. e <sup>-</sup>	16.9465	-1.93452	4.49737	-2.61209	4.84003	0.146590	-1.72196	0	9d
25. H <sup>-</sup>	38.6051	0.677752	-1.60180	1.12449	4.99093	0.148264	0.466771	33229	9d

\*  $G(T) = \Delta H_f(298) - T(A[1] + A[2]X + A[3]X^2 + A[4]X^3 + A[5] \ln(X) + A[6]/X + A[7]X \ln(X))$   
 WHERE  $X = T/10,000$ .

+ See text

Table 3  
(continued)  
Parameters\*

	Species	A[1]	A[2]	A[3]	A[4]	A[5]	A[6]	A[7]	$\Delta H_f$ (298) (ca./mole)	Ref
26.	CsI	87.7432	0.455567	1.98833	-0.530047	8.82342	0.265538	-0.886756	-36305	8
27.	(CsI) <sub>2</sub>	151.730	-0.901373	2.54081	-1.15809	19.6712	0.589180	-1.44663	-109608	8
28.	Cs	55.2284	6.51345	-18.0747	19.4407	5.14409	0.149513	3.91440	18320	9a
29.	Cs <sub>2</sub>	89.1027	-0.253858	5.90677	1.37570	8.68381	0.206196	-3.26444	25400	9a
30.	CsO	78.5451	-7.04194	19.2072	-9.22688	8.00513	0.253281	-8.84657	7000	9a
31.	Cs <sub>2</sub> O	104.008	-11.3324	29.0822	-13.2027	12.0297	0.385426	-15.589	-22000	9a
32.	CsO <sub>2</sub>	72.4901	-51.9515	132.485	-61.5160	5.69640	0.281707	-68.6852	-30003	8
33.	CsOH	88.573	3.27662	7.54214	-7.06251	11.4291	0.354543	-4.25062	-62000	9a
34.	(CsOH) <sub>2</sub>	106.810	23.3675	21.6804	4.44148	12.3878	0.504567	-50.2292	-164400	9a
35.	CsH	58.2397	-18.5988	54.1654	-22.9077	4.60238	0.194397	-31.6596	27653	+
36.	I	54.1543	-6.73066	15.6499	-8.47545	4.60806	0.144204	-5.42569	25517	9c
37.	I <sub>2</sub>	83.0657	-2.01913	6.86623	-3.07306	8.49648	0.260256	-3.68585	14924	9a
38.	HI	69.3864	32.4639	-57.6352	31.3200	7.38825	0.205367	18.0298	5300	9a
39.	CsOH <sup>+</sup>	94.0739	7.49914	-2.99134	-1.93855	12.0113	0.363370	0.949611	106000	9b
40.	CsI <sup>+</sup>	89.3940	-5.08454	14.4769	-7.80608	8.56555	0.262982	-5.09411	133000	+
41.	Cs <sub>2</sub> I <sup>+</sup>	123.266	-1.45445	3.65119	-1.66267	14.6829	0.440980	-1.91171	70000	+
42.	I <sup>+</sup>	55.1837	-6.77894	16.1413	-9.14077	4.76899	0.146829	-4.36665	268026	+
43.	I <sup>-</sup>	53.1044	1.0404	-2.44281	1.62191	5.01230	0.148515	0.769878	-47000	+
44.	Cs <sup>+</sup>	52.5236	-1.93382	4.49575	-2.61117	4.84007	0.146591	-1.72133	109600	9b
45.	Cs <sub>2</sub> <sup>+</sup>	91.4312	2.55877	0.527582	-0.266332	8.91785	0.268733	-0.241853	113163	+
46.	HI <sup>+</sup>	70.7986	26.4370	-40.4586	16.9109	7.43786	0.207530	15.8220	247320	+
47.	I <sub>2</sub> <sup>+</sup>	84.7052	-5.96484	20.2666	-15.4282	8.62056	0.262289	-3.98833	231190	+
48.	I <sub>2</sub> <sup>-</sup>	84.1696	-2.80758	8.71073	-4.07135	8.42830	0.259352	-4.48339	-40868	+

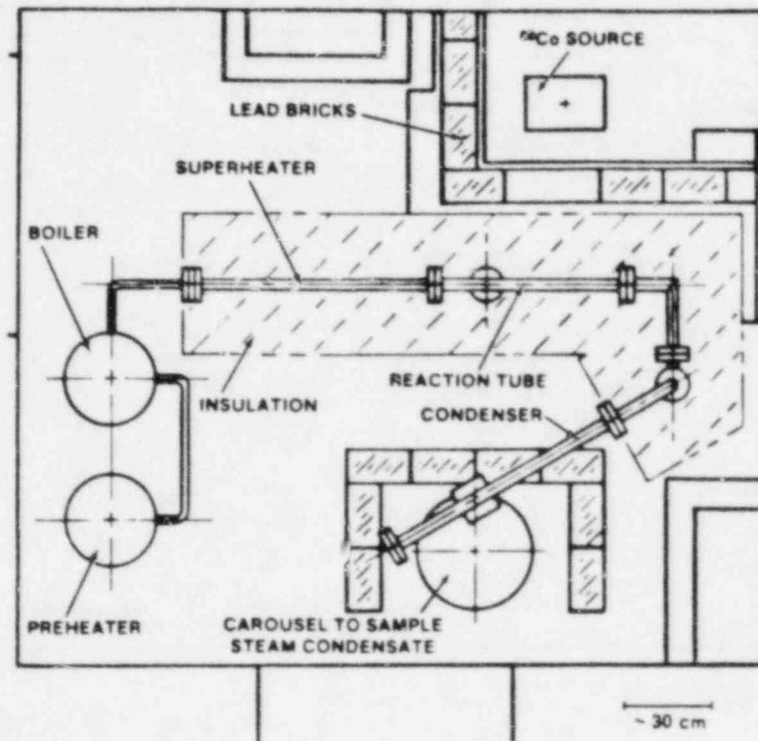


Figure 1. Schematic diagram of the Fission Product Reaction Facility as configured for the tests in a radiation field.

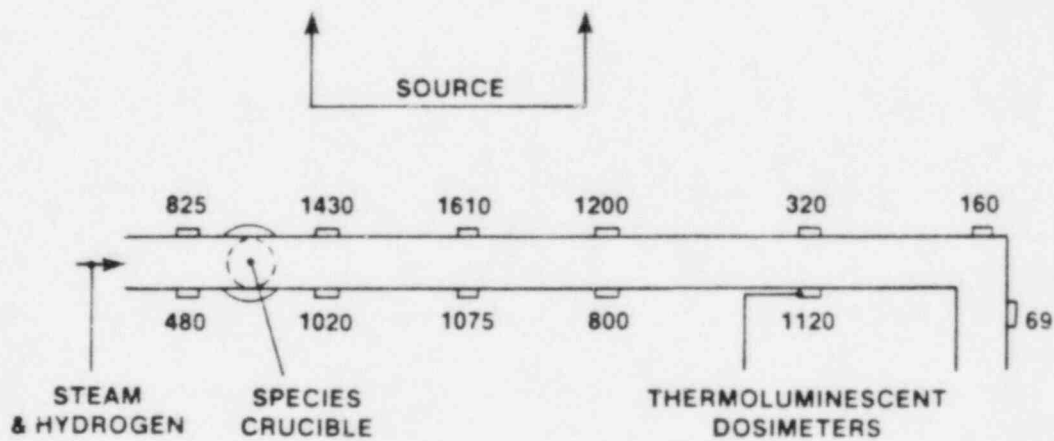


Figure 2. Schematic diagram of dosimetry measurements (rads/min) made for the tests.

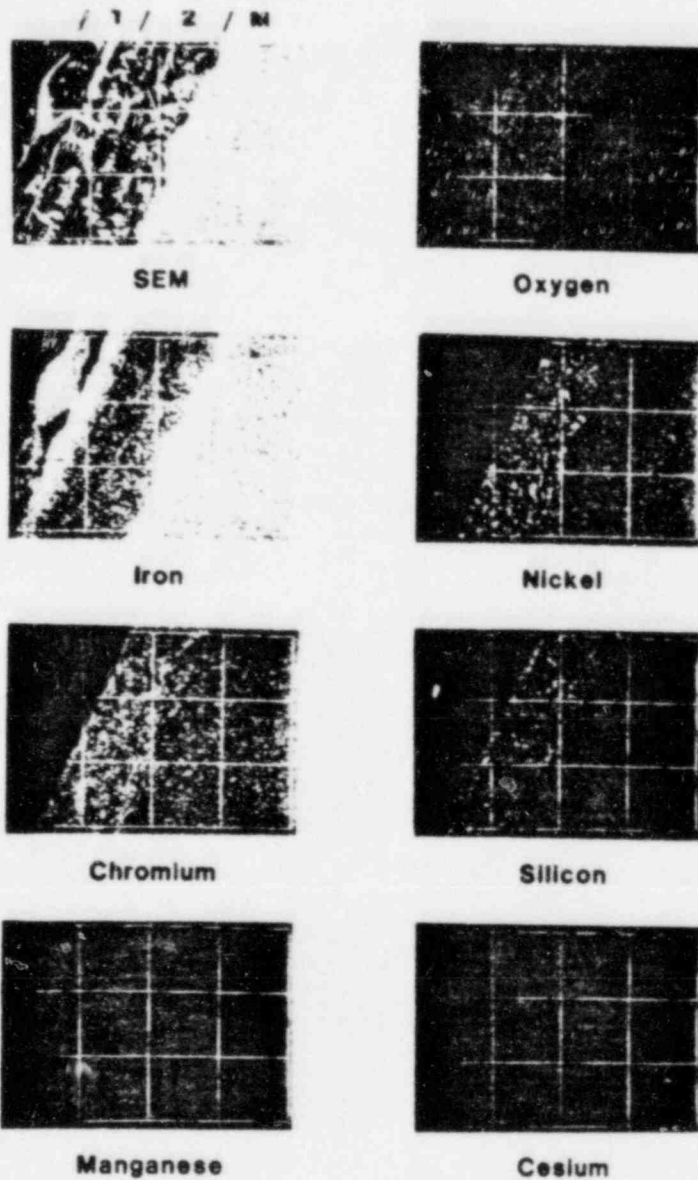


Figure 3. Electron microprobe results for coupons used in test 18 which involved no radiation field. The layers of the duplex oxide are designate 1 and 2. The metal is designated M.

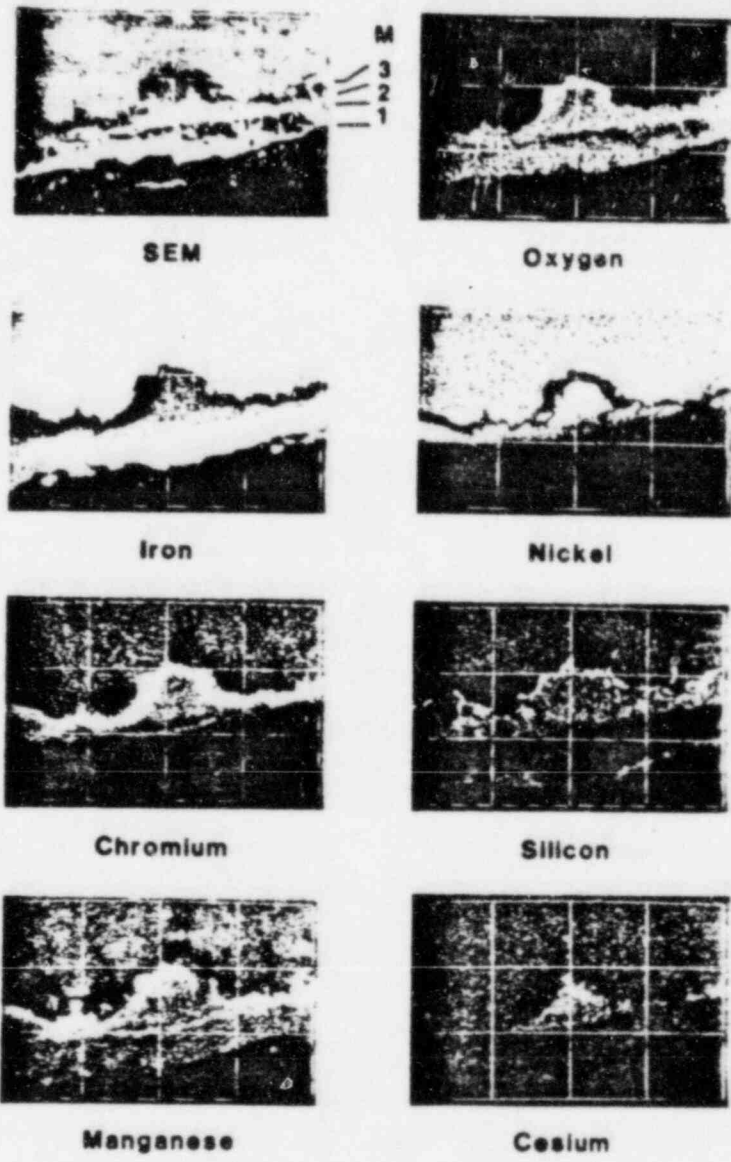


Figure 4. Electron microprobe results for the stainless steel coupon from test 40. The oxide layer is a triplex whose layers are numbered in the SEM photograph.

POINT-BY-POINT MEASUREMENT OF COMPOSITION  
THROUGH OXIDE CROSS SECTION IN TEST 40. CONCENTRATIONS  
CALCULATED FOR CORRESPONDING OXIDE OF ELEMENTS  
 $Mn(MnO_2)$ ,  $Si(SiO_2)$  AND  $Cs(Cs_2O)$

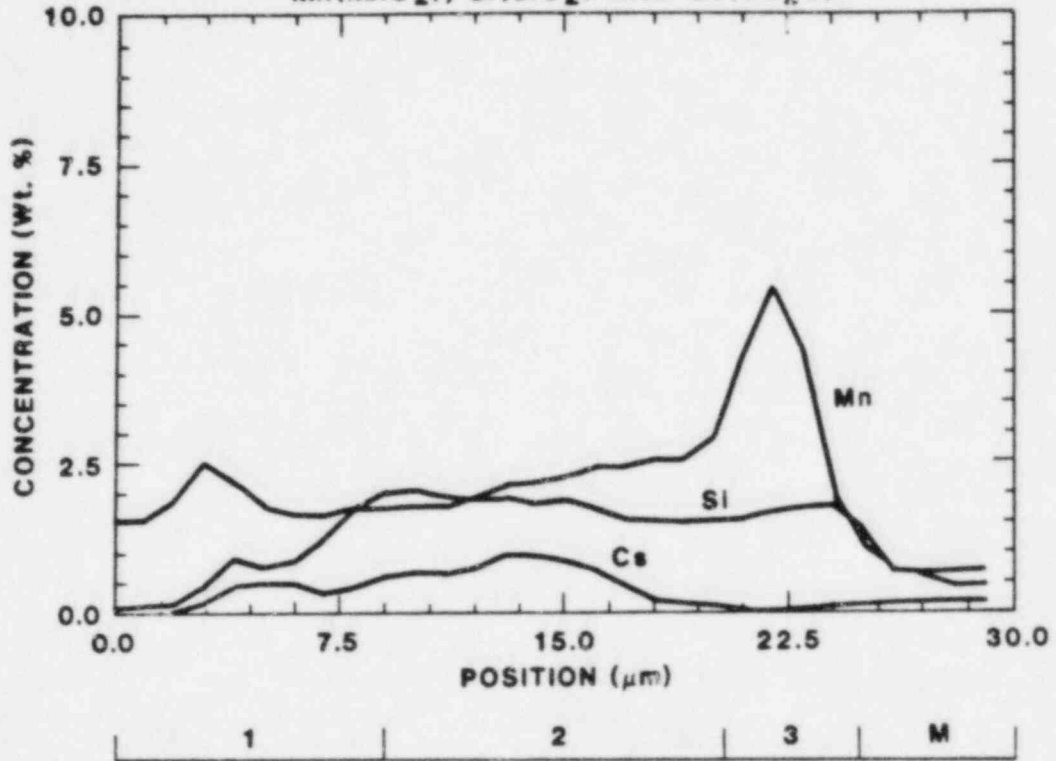


Figure 5. Elemental concentrations plotted against position for the stainless steel coupon from test 40.

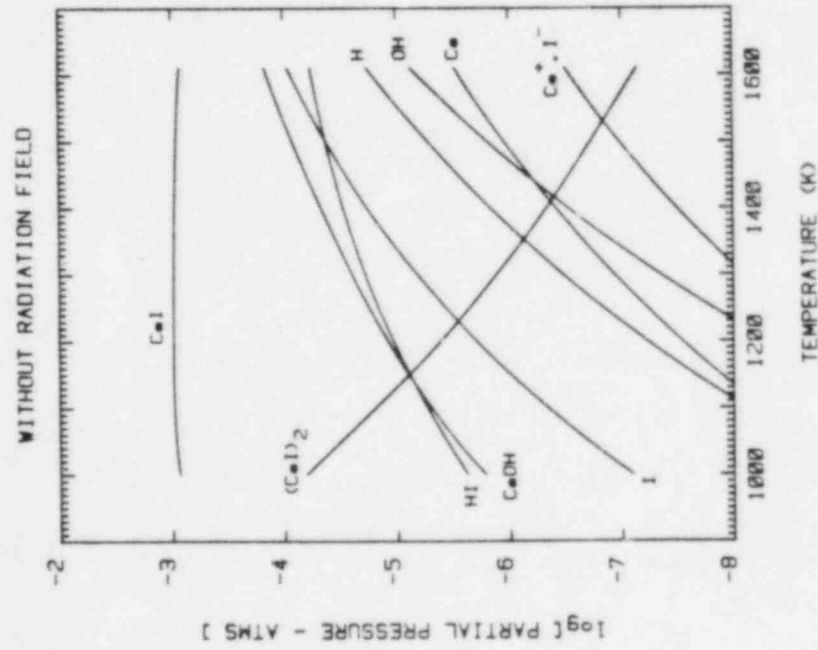
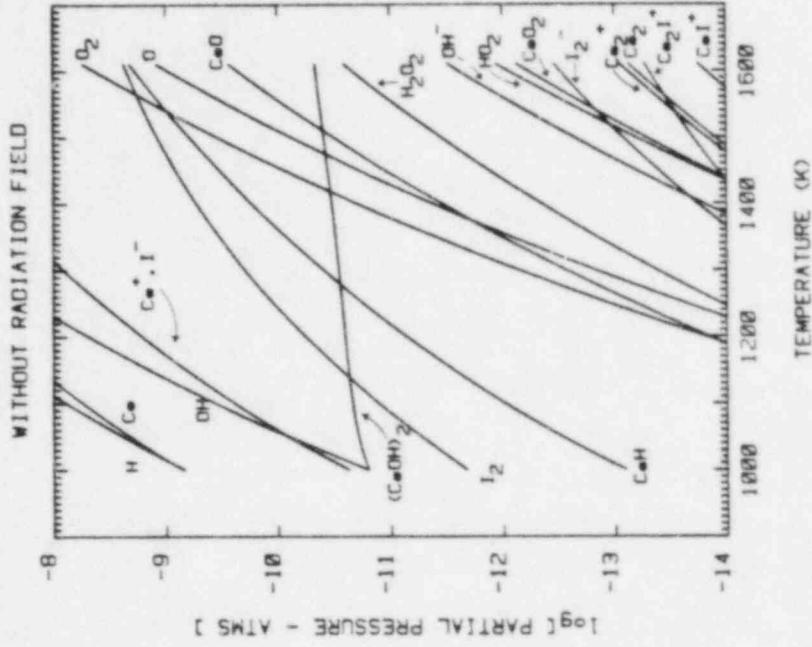


Figure 6. Vapor phase speciation of the Cs-I-O-H system in the absence of a radiation field. Partial pressures of  $H_2O$  and  $H_2$  have not been shown.

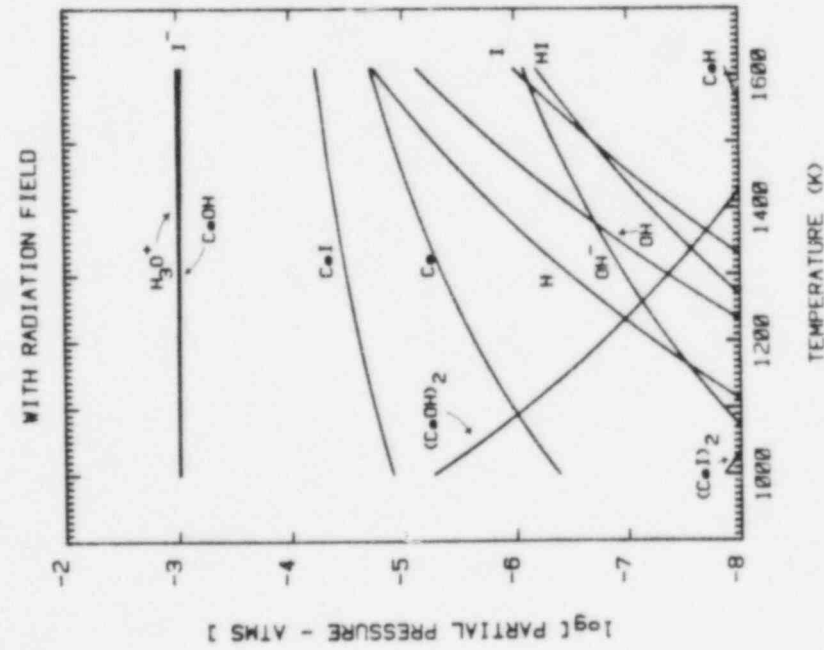
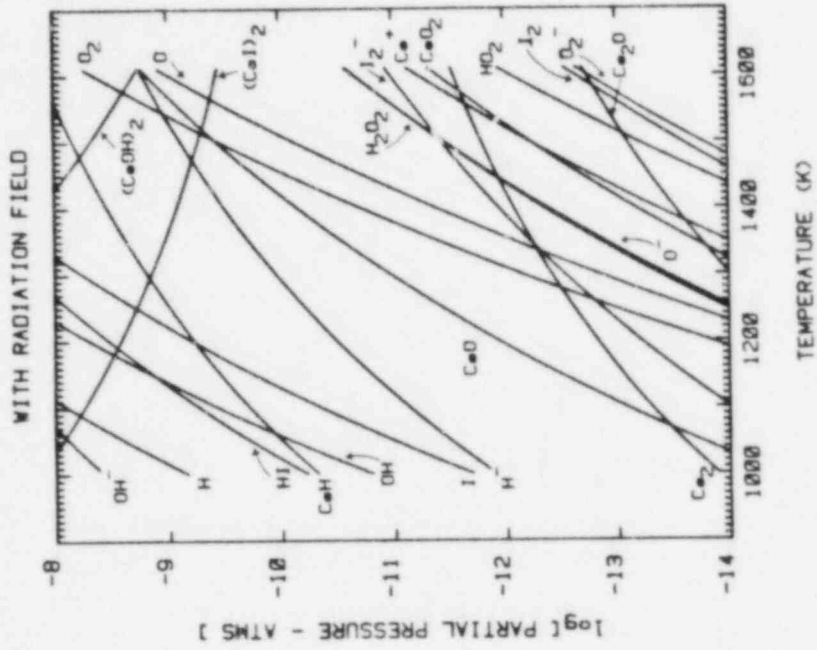


Figure 7. Vapor phase speciation of the Cs-I-O-H system in a radiation field sufficient to produce a dynamic charge separation of  $10^{-3}$ . Partial pressures of  $H_2O(g)$  and  $H_2(\tau)$  have not been indicated.